M&C 2023 - The International Conference on Mathematics and Computational Methods Applied to Nuclear Science and Engineering · Niagara Falls, Ontario, Canada · August 13 – 17, 2023

A "Consistent" Quasidiffusion Method for Iteratively Solving Particle Transport Problems

E.W. Larsen[1], T.M. Paganin[2], R. Vasques[2]

[1]Department of Nuclear Engineering and Radiological Sciences,
University of Michigan, Ann Arbor, MI 48104

[2] Department of Mechanical and Aerospace Engineering,
Ohio State University, Columbus, OH 43210

edlarsen@umich.edu,mallmannpaganin.1@osu.edu,vasques.4@osu.edu

ABSTRACT

The "Quasidiffusion" (QD) method is a well-known iterative technique for efficiently solving particle transport problems. Each QD iteration consists of a high-order S_N sweep, followed by a low-order "Quasidiffusion" calculation. QD has two defining characteristics: (i) its iterations converge rapidly for any spatial grid, and (ii) the converged scalar fluxes from the high-order S_N sweep and the low-order Quasidiffusion calculation differ – by spatial truncation errors – from each other, and from the scalar flux solution of the S_N equations. In this paper we show that by including a *transport consistency factor* in the low-order QD equation, the converged high-order and low-order QD scalar fluxes become equal to each other, and to the converged S_N scalar flux. We also present CQD numerical results to demonstrate the effect of the transport consistency factor on stability.

KEYWORDS: neutron transport, iteration, acceleration

1. INTRODUCTION

The *Quasidiffusion* (QD) method is an established iterative method for solving particle transport problems [1–3]. (In the Astrophysical community, QD is widely-used and usually called the *Variable Eddington Factor* (VEF) method.) Each QD iteration has two parts: a high-order S_N sweep using a scattering source estimated from the previous iteration, followed by a low-order "Quasidiffusion" calculation containing an Eddington factor estimated from the S_N sweep. The discretized QD method converges rapidly for any choice of spatial grid. However, the converged high-order and low-order scalar fluxes, and the scalar flux obtained by solving the S_N equations, all differ by spatial truncation errors. Thus, QD is not a true *acceleration* method: its converged scalar fluxes differ from the scalar flux calculated from the converged angular flux solution of the S_N equations. In this paper, we show that by including a *transport consistency factor* in the discretized low-order QD equations, the converged high-order transport and low-order QD scalar fluxes become equal to each other, and to the S_N scalar flux. The new consistency factor is formally small – it is $O(\Sigma_t h)^2$. Setting this factor to zero introduces a second-order Quaisdiffusion error and yields the familiar inconsistent QD method. Keeping this factor, we obtain the new *Consistent Quasidiffusion* (CQD) method, which is a true transport acceleration method, such as *Diffusion Synthetic Acceleration* (DSA) [3] and *Coarse Mesh Finite Difference* (CMFD) [4,5]. This paper includes numerical results from implementing and testing the CQD method in a 1-D S_N code.

Modifications of QD that make it a true acceleration method have been proposed in two earlier publications [6,7]. In this previous work, the low-order QD equations are modified in ways that require the calculation and storage of cell-edge scalar flux estimates. Our simpler CQD method does not require such calculations, and is closely-related to the well-known *Coarse Mesh Finite Difference* (CMFD) and *Diffusion Synthetic Acceleration* (DSA) methods [3–5]. (The derivation of CQD in this paper demonstrates the close theoretical link between CQD and CMFD.)

Unfortunately, the inclusion of the CQD transport consistency factor has a harmful effect on the stability of the method. We have implemented and tested the CQD method in a 1-D S_N code, and we present numerical results from this code in this paper. Our results show that the CQD and CMFD methods have nearly the same stability properties: they both converge rapidly for problems with optically thin spatial cells, but they degrade at nearly the same rate as the spatial cells increase in optical thickness. Currently, we are experimenting with different ideas to try to ameliorate this difficulty. In future work, we plan to develop a Fourier stability analysis, to theoretically predict the spectral radius of the CQD method and validate our experimental results.

Although the stability properties of CQD are disappointing compared to those of QD, the results in this paper are still potentially useful. These results show that with minimal effort, a QD (or VEF) code can be modified to include the CQD method, and thereby become "consistent." There are situations in which this capability could be useful. For one example, if a problem that is considered mostly suitable for QD contains "transport" regions, in which the QD approximation might be inaccurate, it would be possible to run this problem with the CQD method turned on, to assess whether the transport effects are significant. A second example would be setting the CQD transport consistency factor equal to zero in "diffusive" regions of the problem (the QD approximation), but retaining the consistency factor in "transport" regions. In general, the ability to fully or partially convert a QD code to a CQD code could add meaningful computational flexibility to the code.

The remainder of this paper is organized as follows. Section 2 contains theoretical derivations of the QD, CMFD, and CQD methods. Section 3 contains computational results from the implementation of the QD, CMFD, and CQD methods in our 1-D S_N test code. The final Section 4 includes a summary and discussion.

2. THEORY

Using standard notation, we consider (i) the following 1-D, fixed-source, monoenergetic, spatially discrete, isotropically-scattering S_N equations:

$$\frac{\mu_n}{h_j}\left(\psi_{n,j+\frac{1}{2}} - \psi_{n,j-\frac{1}{2}}\right) + \Sigma_{t,j}\psi_{n,j} = \frac{\Sigma_{s,j}}{2}\sum_{n'=1}^{N}\psi_{n',j}w_{n'} + \frac{Q_j}{2}\ , \tag{1a}$$

$$\psi_{n,j} = \left(\frac{1+\alpha_{n,j}}{2}\right)\psi_{n,j+\frac{1}{2}} + \left(\frac{1-\alpha_{n,j}}{2}\right)\psi_{n,j-\frac{1}{2}}\ , \tag{1b}$$

which hold for $1 \leq j \leq J$ and $1 \leq n \leq N$, and (ii) prescribed incident flux boundary conditions:

$$\psi_{n,\frac{1}{2}} = \Psi_n^l\ ,\ \mu_n > 0\ , \tag{1c}$$

$$\psi_{n,J+\frac{1}{2}} = \Psi_n^r\ ,\ \mu_n < 0\ . \tag{1d}$$

In the following, we derive the CQD method for Eqs. (1).

First, we operate on Eq. (1a) by $\sum_{n=1}^{N}(\cdot)w_n$ and define the cell-average and cell-edge angular flux moments:

$$\phi_{k,j} = \sum_{n=1}^{N}(\mu_n)^k\psi_{n,j}w_n\ \ ,\ \ \phi_{k,j+\frac{1}{2}} = \sum_{n=1}^{N}(\mu_n)^k\psi_{n,j+\frac{1}{2}}w_n\ , \tag{2}$$

to obtain the familiar neutron balance equation:

$$\frac{1}{h_j}\left(\phi_{1,j+\frac{1}{2}} - \phi_{1,j-\frac{1}{2}}\right) + \Sigma_{a,j}\phi_{0,j} = Q_j\ , \tag{3}$$

where $\Sigma_{a,j} = \Sigma_{t,j} - \Sigma_{s,j}$. Also, we multiply Eqs. (1c) and (1d) by $|\mu_n|w_n$ and sum each equation over the

incident directions of flight, to obtain the partial currents:

$$\sum_{\mu_n>0} \mu_n \psi_{n,\frac{1}{2}} w_n = \sum_{\mu_n>0} \mu_n \Psi^l_n w_n \equiv \mathcal{J}^+_l \ , \tag{4a}$$

$$\sum_{\mu_n<0} |\mu_n| \psi_{n,J+\frac{1}{2}} w_n = \sum_{\mu_n<0} |\mu_n| \Psi^r_n w_n \equiv \mathcal{J}^-_r \ . \tag{4b}$$

We also operate on Eq. (1a) by $\sum_{n=1}^N \mu_n(\cdot) w_n$ and rearrange to obtain the identity:

$$\begin{aligned} \phi_{1,j} &= -\frac{1}{\Sigma_{t,j} h_j} \left(\phi_{2,j+\frac{1}{2}} - \phi_{2,j-\frac{1}{2}} \right) \\ &= -\frac{1}{\Sigma_{t,j} h_j} \left(E_{j+\frac{1}{2}} \phi_{0,j+\frac{1}{2}} - E_{j-\frac{1}{2}} \phi_{0,j-\frac{1}{2}} \right) \ , \end{aligned} \tag{5a}$$

which is "centered" on cell j. In Eq. (5a) we have introduced the *cell-edge Eddington factor:*

$$E_{j+\frac{1}{2}} = \frac{\phi_{2,j+\frac{1}{2}}}{\phi_{0,j+\frac{1}{2}}} \ . \tag{5b}$$

Eqs. (5) are satisfied by the converged solution of the S_N equations.

The CQD method utilizes an identity that is similar to Eqs. (5), but instead is "centered" on cell edges:

$$\phi_{1,j+\frac{1}{2}} = -\frac{1}{(\Sigma_t h)_{j+\frac{1}{2}}} \left(E_{j+1} \phi_{0,j+1} - E_j \phi_{0,j} \right) + \tilde{D}_{j+\frac{1}{2}} \left(\phi_{0,j+1} + \phi_{0,j} \right) \ , \tag{6a}$$

where:

$$(\Sigma_t h)_{j+\frac{1}{2}} = \frac{1}{2} \left(\Sigma_{t,j+1} h_{j+1} + \Sigma_{t,j} h_j \right) \ , \tag{6b}$$

$$E_j = \frac{\phi_{2,j}}{\phi_{0,j}} = \text{cell-average Eddington factor} \ , \tag{6c}$$

and $\tilde{D}_{j+\frac{1}{2}}$ is a dimensionless *transport consistency factor*:

$$\tilde{D}_{j+\frac{1}{2}} = \frac{\phi_{1,j+\frac{1}{2}} + \frac{1}{(\Sigma_t h)_{j+\frac{1}{2}}} \left(\phi_{2,j+1} - \phi_{2,j} \right)}{\phi_{0,j+1} + \phi_{0,j}} \ . \tag{6d}$$

Like Eqs. (5), Eqs. (6) are satisfied by the converged solution of the S_N equations. Because of Eq. (5a), the consistency factor $\tilde{D}_{j+\frac{1}{2}}$ is formally $O(\Sigma_t h)^2$ – it vanishes as the optical width of a spatial cell limits to zero. The CQD method assumes that $\tilde{D}_{j+\frac{1}{2}}$ is sufficiently small that, when it is used in an iterative scheme, it can be lagged.

The CQD method also uses identities derived from the "boundary" Eqs. (4). Eq. (4a) is written as:

$$\begin{aligned} 2\mathcal{J}^+_l &= \sum_{\mu_n>0} 2\mu_n \psi_{n,\frac{1}{2}} w_n \\ &= \sum_{n=1}^N (\mu_n + |\mu_n|) \psi_{n,\frac{1}{2}} w_n \\ &= \sum_{n=1}^N \mu_n \psi_{n,\frac{1}{2}} w_n + \sum_{n=1}^N |\mu_n| \psi_{n,\frac{1}{2}} w_n \\ &= \phi_{1,\frac{1}{2}} + \left(\frac{\sum_{n=1}^N |\mu_n| \psi_{n,\frac{1}{2}} w_n}{\phi_{0,1}} \right) \phi_{0,1} \\ &\equiv \phi_{1,\frac{1}{2}} + B_l \phi_{0,1} \ , \end{aligned} \tag{7a}$$

where

$$B_l = \frac{\sum_{n=1}^{N} |\mu_n| \psi_{n,\frac{1}{2}} w_n}{\phi_{0,1}} \ . \tag{7b}$$

Similarly, Eq. (4b) is written as:

$$2\mathcal{J}_r^- = -\phi_{1,J+\frac{1}{2}} + B_r \phi_{0,J} \ , \tag{8a}$$

where

$$B_r = \frac{\sum_{n=1}^{N} |\mu_n| \psi_{n,J+\frac{1}{2}} w_n}{\phi_{0,J}} \ . \tag{8b}$$

(The *boundary factors* B_l and B_r are similar to the Eddington factors. They are assumed to be "stable" in value from one iteration to the next, and in the CQD method they are lagged.)

At the beginning of the $(\ell+1)^{st}$ CQD iteration, a scalar flux estimate $\phi_{0,j}^{\ell}$ is known from the previous ℓ^{th} iteration (or is assigned if $\ell = 0$). The first part of the CQD iteration consists of a transport sweep, in which $\phi_{0,j}^{\ell}$ is used to estimate the scattering source, and then certain cell-average and cell-edge flux moments are calculated and stored. From Eqs. (1) and (2), these operations are defined by:

$$\frac{\mu_n}{h_j}\left(\psi_{n,j+\frac{1}{2}}^{\ell+\frac{1}{2}} - \psi_{n,j-\frac{1}{2}}^{\ell+\frac{1}{2}}\right) + \Sigma_{t,j}\psi_{n,j}^{\ell+\frac{1}{2}} = \frac{\Sigma_{s,j}}{2}\phi_{0,j}^{\ell} + \frac{Q_j}{2} \ , \tag{9a}$$

$$\psi_{n,j}^{\ell+\frac{1}{2}} = \left(\frac{1+\alpha_{n,j}}{2}\right)\psi_{n,j+\frac{1}{2}}^{\ell+\frac{1}{2}} + \left(\frac{1-\alpha_{n,j}}{2}\right)\psi_{n,j-\frac{1}{2}}^{\ell+\frac{1}{2}} \ , \tag{9b}$$

$$\psi_{n,\frac{1}{2}}^{\ell+\frac{1}{2}} = \Psi_n^l \ , \ \ \mu_n > 0 \ , \tag{9c}$$

$$\psi_{n,J+\frac{1}{2}}^{\ell+\frac{1}{2}} = \Psi_n^r \ , \ \ \mu_n < 0 \ , \tag{9d}$$

and:

$$\phi_{k,j}^{\ell+\frac{1}{2}} = \sum_{n=1}^{N} \mu_n^k \psi_{n,j}^{\ell+\frac{1}{2}} w_n \ \ (k=0,2) \quad , \quad \phi_{1,j+\frac{1}{2}}^{\ell+\frac{1}{2}} = \sum_{n=1}^{N} \mu_n \psi_{n,j+\frac{1}{2}}^{\ell+\frac{1}{2}} w_n \ , \tag{10a}$$

$$\phi_{|1|,\frac{1}{2}}^{\ell+\frac{1}{2}} \equiv \sum_{n=1}^{N} |\mu_n| \psi_{n,\frac{1}{2}}^{\ell+\frac{1}{2}} w_n \quad , \quad \phi_{|1|,J+\frac{1}{2}}^{\ell+\frac{1}{2}} \equiv \sum_{n=1}^{N} |\mu_n| \psi_{n,J+\frac{1}{2}}^{\ell+\frac{1}{2}} w_n \ . \tag{10b}$$

In the second "low-order" part of a CQD iteration, the estimates from Eqs. (10) are used to determine new estimates of the cell-averaged Eddington factors [Eq. (6c)], the transport consistency factors [Eq. (6d)], and the boundary factors [Eqs. (7b) and (8b)]:

$$E_j^{\ell+\frac{1}{2}} = \frac{\phi_{2,j}^{\ell+\frac{1}{2}}}{\phi_{0,j}^{\ell+\frac{1}{2}}} \quad , \quad \tilde{D}_{j+\frac{1}{2}}^{\ell+\frac{1}{2}} = \frac{\phi_{1,j+\frac{1}{2}}^{\ell+\frac{1}{2}} + \frac{1}{(\Sigma_t h)_{j+\frac{1}{2}}}\left(\phi_{2,j+1}^{\ell+\frac{1}{2}} - \phi_{2,j}^{\ell+\frac{1}{2}}\right)}{\phi_{0,j+1}^{\ell+\frac{1}{2}} + \phi_{0,j}^{\ell+\frac{1}{2}}} \ , \tag{11a}$$

$$B_l^{\ell+\frac{1}{2}} = \frac{\phi_{|1|,\frac{1}{2}}^{\ell+\frac{1}{2}}}{\phi_{0,1}^{\ell+\frac{1}{2}}} \quad , \quad B_r^{\ell+\frac{1}{2}} = \frac{\phi_{|1|,J+\frac{1}{2}}^{\ell+\frac{1}{2}}}{\phi_{0,J}^{\ell+\frac{1}{2}}} \ . \tag{11b}$$

These are introduced in Eqs. (3), (6a), (7a), and (8a), yielding the following discrete linear system of equations for the cell-edge scalar fluxes and the cell-edge currents:

$$\frac{1}{h_j}\left(\phi^{\ell+1}_{1,j+\frac{1}{2}} - \phi^{\ell+1}_{1,j-\frac{1}{2}}\right) + \Sigma_{a,j}\phi^{\ell+1}_{0,j} = Q_j \ , \tag{12a}$$

$$\phi^{\ell+1}_{1,j+\frac{1}{2}} = -\frac{1}{(\Sigma_t h)_{j+\frac{1}{2}}}\left(E^{\ell+\frac{1}{2}}_{j+1}\phi^{\ell+1}_{0,j+1} - E^{\ell+\frac{1}{2}}_{j}\phi^{\ell+1}_{0,j}\right) + \tilde{D}^{\ell+\frac{1}{2}}_{j+\frac{1}{2}}\left(\phi^{\ell+1}_{0,j+1} + \phi^{\ell+1}_{0,j}\right) \ , \tag{12b}$$

$$\phi^{\ell+1}_{1,\frac{1}{2}} = 2\mathcal{J}^{+}_{l} - B^{\ell+\frac{1}{2}}_{l}\phi^{\ell+1}_{0,1} \ , \tag{12c}$$

$$\phi^{\ell+1}_{1,J+\frac{1}{2}} = -2\mathcal{J}^{-}_{r} + B^{\ell+\frac{1}{2}}_{r}\phi^{\ell+1}_{0,J} \ . \tag{12d}$$

[Eqs. (12a) hold for $1 \le j \le J$, and Eqs. (12b) hold for $1 \le j \le J-1$.] Eqs. (12b), (12c), and (12d) enable the cell-edge currents to be eliminated from Eqs. (12a), yielding an easily-solved linear tridiagonal system of "CQD" equations for the cell-averaged scalar fluxes $\phi^{\ell+1}_{0,j}$. The inclusion of the consistency factors in Eq. (12b) ensures that if the CQD method converges, the converged high-order and low-order CQD scalar fluxes will equal the converged S_N scalar fluxes.

This completes our derivation of the CQD method. Next, we show how this method relates to the standard Quasidiffusion (QD) and the Coarse Mesh Finite Difference (CMFD) methods.

The standard QD method is obtained from CQD by setting, in Eqs. (12b), the transport consistency factors equal to zero:

$$\tilde{D}^{\ell+\frac{1}{2}}_{j+\frac{1}{2}} = 0 \ . \tag{13}$$

The consistency factors are formally $O(\Sigma_t h)^2$; setting them to zero introduces a second-order truncation error that drives the high-order scalar flux estimates in Eqs. (10a), and the low-order scalar flux estimates in Eqs. (12), away from each other and from the converged scalar flux solution of the S_N equations. (The inclusion of the CQD consistency factors prevents the "contamination" of the S_N solution.)

The CQD method derived in this paper is closely-related to the CMFD method for the case in which the high-order and low-order spatial grids are equal. (This special case of CMFD is sometimes called "Nonlinear Diffusion Acceleration" (NDA), but we simply call it CMFD here. The CQD method can easily be generalized to the case of a coarser low-order spatial grid, but this is not done in the present paper.)

The CQD method is based on the identity expressed in Eqs. (6). The CMFD method (with fine-grid equal to the coarse-grid) is based on the following similar identity:

$$\phi_{1,j+\frac{1}{2}} = -\frac{1}{3(\Sigma_t h)_{j+\frac{1}{2}}}\left(\phi_{0,j+1} - \phi_{0,j}\right) + \hat{D}_{j+\frac{1}{2}}\left(\phi_{0,j+1} + \phi_{0,j}\right) \ , \tag{14a}$$

$$\hat{D}_{j+\frac{1}{2}} = \frac{\phi_{1,j+\frac{1}{2}} + \frac{1}{3(\Sigma_t h)_{j+\frac{1}{2}}}\left(\phi_{0,j+1} - \phi_{0,j}\right)}{\phi_{0,j+1} + \phi_{0,j}} \ . \tag{14b}$$

Here, $\hat{D}_{j+\frac{1}{2}}$ is a different transport consistency factor; its definition is based on the assumption that Fick's Law:

$$\phi_{1,j+\frac{1}{2}} \approx -\frac{1}{3(\Sigma_t h)_{j+\frac{1}{2}}}\left(\phi_{0,j+1} - \phi_{0,j}\right) \tag{15}$$

is valid, and consequently that $\hat{D}_{j+\frac{1}{2}}$ is small (and can be lagged). The CMFD method is obtained by replacing Eq. (12b) by:

$$\phi^{\ell+1}_{1,j+\frac{1}{2}} = -\frac{1}{(3\Sigma_t h)_{j+\frac{1}{2}}}\left(\phi^{\ell+1}_{0,j+1} - \phi^{\ell+1}_{0,j}\right) + \hat{D}^{\ell+\frac{1}{2}}_{j+\frac{1}{2}}\left(\phi^{\ell+1}_{0,j+1} + \phi^{\ell+1}_{0,j}\right) \ , \tag{16a}$$

where

$$\hat{D}_{j+\frac{1}{2}}^{\ell+\frac{1}{2}} = \frac{\phi_{1,j+\frac{1}{2}}^{\ell+\frac{1}{2}} + \frac{1}{(3\Sigma_t h)_{j+\frac{1}{2}}}\left(\phi_{0,j+1}^{\ell+\frac{1}{2}} - \phi_{0,j}^{\ell+\frac{1}{2}}\right)}{\phi_{0,j+1}^{\ell+\frac{1}{2}} + \phi_{0,j}^{\ell+\frac{1}{2}}} \,. \tag{16b}$$

Note: In the CMFD method, no changes are made to the boundary conditions Eqs. (12c) and (12d).

The CQD method is premised on the concept that the CQD consistency factor [Eq. (11a)] is sufficiently resolved by the spatial grid that it is small and can be lagged, while the CMFD method is premised on the idea that Fick's Law is sufficiently satisfied that the CMFD transport consistency factor [Eq. (14b)] is sufficiently small and can be lagged. Because Fick's Law is not inherently satisfied by the solution of a transport problem, it is plausible that the CMFD consistency factor may be larger than the simple CQD consistency factor, and hence that CMFD will be less stable than CQD. (This motivated our work on the CQD method.) This hope turned out to be somewhat premature, as we discuss next.

3. NUMERICAL RESULTS

We have implemented the Source Iteration (SI), CMFD, QD, and CQD methods in a 1-D test code and compared these methods applied to several different problems. Our results are presented below.

Problem 1 is designed to demonstrate that (i) the SI, CMFD, and CQD methods are encoded correctly, and (ii) the QD method produces different scalar fluxes. The physical system is a slab $0 < x < 25$ cm with

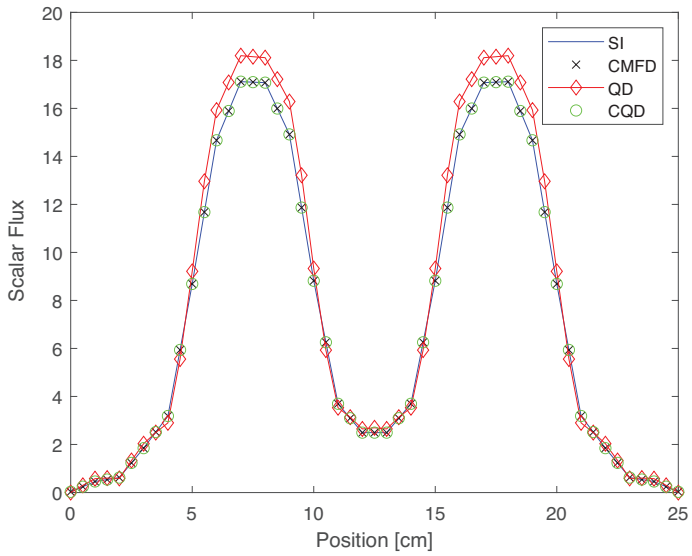

Figure 1: QD and S_N Scalar Fluxes for Problem 1

vacuum boundaries. The system has five subregions, each 5 cm thick. Going from left to right, subregions 1, 3, and 5 have $\Sigma_t = 1.0$ cm^{-1}, $\Sigma_s = 0.9$ cm^{-1}, and $Q = 0$ cm^{-3} sec^{-1}. Subregions 2 and 4 have $\Sigma_t = 1.0$ cm^{-1}, $\Sigma_s = 0.99$ cm^{-1}, and $Q = 1.0$ cm^{-3} sec^{-1}. This problem is symmetric about its midpoint, $x = 25.0$. We ran the problem using (i) the standard S_{32} Gauss-Legendre quadrature set, (ii) a spatial grid with uniform spatial cells of thickness $h = 1.0$ cm, and (iii) a convergence criterion of 10^{-9}. The resulting scalar fluxes are plotted in Figure 1. The numerical values of the SI, CMFD, and CQD scalar fluxes agreed to within the 10^{-9} convergence criterion, and the QD scalar fluxes differed from these by small but significant amounts. The numerical solutions were all symmetric about the midpoint $x = 25$. (We include this plot as evidence that our test code was properly debugged.)

Problems 2, 3, and 4 were designed to assess the effect of the transport correction factor on the stability of CQD, and to compare this stability to that of CMFD. Problem 2 is a homogeneous slab of variable thickness $0 \leq x \leq X = 100h$, where h is the (variable) width of a spatial cell. (The system is always $J = 100$ cells thick.) The boundaries are vacuum, and within the system, $\Sigma_t = 1.0$ cm^{-1}, $\Sigma_s = 0.99$ cm^{-1}, and $Q = 1.0$ cm^{-3} sec^{-1}. We used the S_{32} quadrature set with a convergence criterion of 10^{-9}.

Assessing the effect of the spatial cell width h on the rate of convergence of the CQD (and CMFD) methods can be done by estimating the spectral radius. To do this, we calculate the L_2 norm of the difference between the cell-averaged scalar flux estimates from successive iterates:

$$||\phi^{\ell+1} - \phi^{\ell}|| \equiv \left(\frac{\sum_{j=1}^{J} |\phi_j^{\ell+1} - \phi_j^{\ell}|^2 h_j}{\sum_{j=1}^{J} h_j} \right)^{1/2} , \tag{17a}$$

and then we estimate the spectral radius ρ by calculating the ratio

$$\rho \approx \frac{||\phi^{\ell+1} - \phi^{\ell}||}{||\phi^{\ell} - \phi^{\ell-1}||} . \tag{17b}$$

A method converges if and only if $\rho < 1$, in which case right side of Eq. (17b) converges as $\ell \to \infty$ to the asymptotic error reduction per iteration – the spectral radius. In Figure 2 below, we plot, for the CMFD and CQD methods, the numerically-estimated spectral radius versus the optical cell width $\Sigma_t h$ for Problem 2.

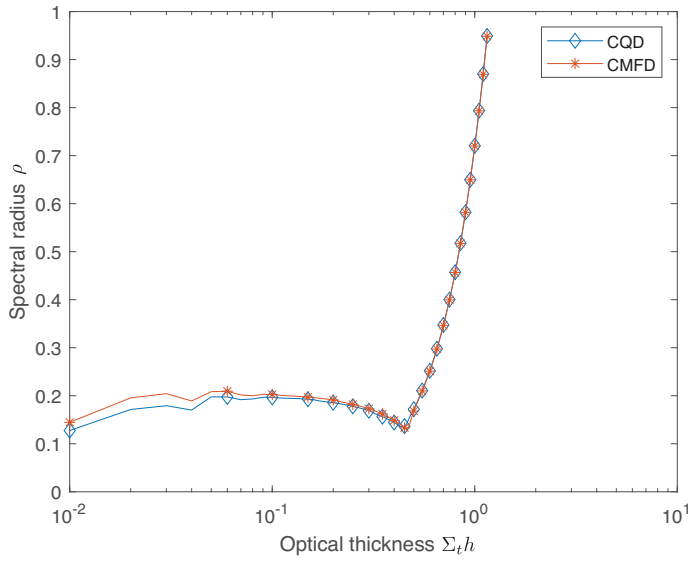

Figure 2: ρ vs $\Sigma_t h$ for Problem 2 ($c = 0.99$)

For this problem, the CMFD and CQD methods have remarkably similar stability properties. Both methods are stable and converge rapidly for optically thin spatial cells. However, as the optical thickness of cells increases to about 1 mean free path, both methods degrade and eventually become unstable.

Problem 3 is similar to Problem 2. The only changes are that $\Sigma_s = 0.999$ cm^{-1}, and the internal source is now space-dependent:

$$Q(x) = \begin{cases} 0 & , \quad 0 < x < \frac{X}{2} , \\ 1 & , \quad \frac{X}{2} < x < X . \end{cases} \tag{18}$$

The plot of ρ versus $\Sigma_t h$ is similar to that of Problem 2:

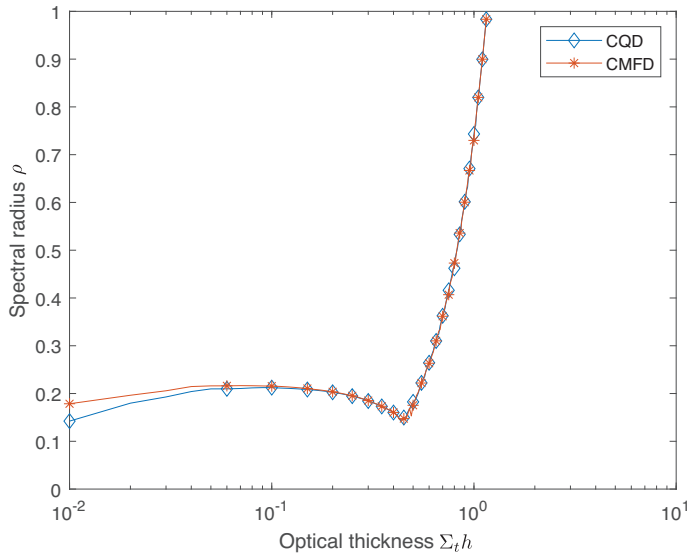

Figure 3: ρ vs $\Sigma_t h$ for Problem 3 ($c = 0.999$)

Unlike Problems 2 and 3, which are driven by internal sources, Problem 4 is driven by a boundary source. The parameters of Problem 4 are the same as Problem 2, except that now Σ_s = 0.9999 cm^{-1}, $Q(x) = 0$, and an isotropic flux is incident on the left boundary. The plot of ρ versus $\Sigma_t h$ is similar to that of Problems 2 and 3:

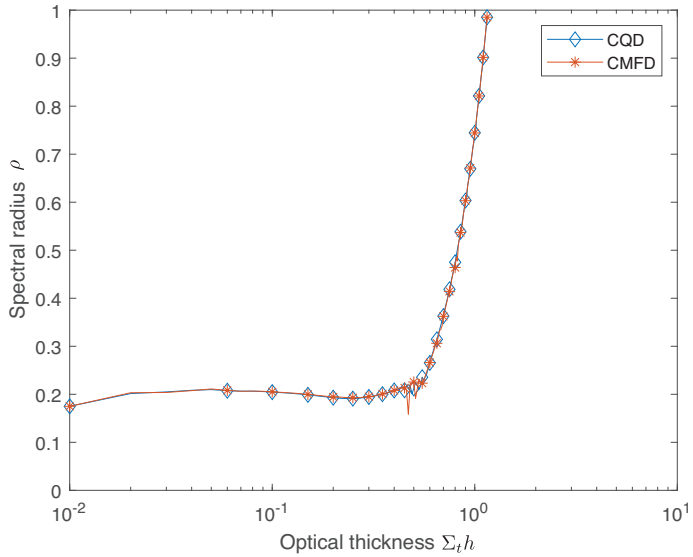

Figure 4: ρ vs $\Sigma_t h$ for Problem 4 ($c = 0.9999$)

Overall, the plots in Figures 2, 3, and 4 indicate that the CQD spectral radius is remarkably similar to the CMFD spectral radius. (We have tested our code on numerous other problems, some with smaller values of the scattering ratio; for each problem, we saw this same result.) It has been known for years that CMFD is stable for problems with optically thin spatial cells $\Sigma_t h \ll 1$, but degrades as $\Sigma_t h$ increases. Our

experimental results (i) confirm this CMFD behavior, and (ii) show that CQD has nearly identical behavior. These experimental results lead us to conjecture that if an infinite-medium linearized Fourier analysis of the CQD method were performed, it would yield the same estimate of the spectral radius as the same analysis applied to CMFD [5]. We hope to perform this analysis in future work.

4. DISCUSSION

We have shown that by including a *transport consistency factor* in the low-order Quasidiffusion equation, one can convert the inconsistent QD method into a consistent CQD method, which preserves the discretized scalar flux solution of the S_N equations. Unfortunately, this consistency factor degrades the stability of the method. The original QD method is unconditionally stable for problems with any size spatial grid – provided the angular fluxes do not become negative (this can introduce an instability in the nonlinear Eddington factors). The CQD method is stable for problems with optically thin spatial cells, but – just like CMFD – CQD degrades in performance and eventually becomes unstable when the spatial cells become greater than about one mean free path thick.

The instability in CQD is not caused by the Eddington or boundary factors – it is caused by the transport consistency factors, which upon convergence are small [they are $O(\Sigma_t h)^2$]. It seems strange to us that the "small" transport consistency term has such a significant effect on stability. We are investigating alternate ways in which this term could be treated, to possibly improve the stability of the method.

For simplicity, the CQD method derived in this paper used the same spatial grid for the low-order Quasidiffusion equation that was used for the high-order S_N equations. However, it is straightforward to generalize the CQD method to problems in which the low-order diffusion grid is coarser than the high-order grid, with cross sections that are homogenized (flux-weighted) over the coarse spatial cells. This procedure is widely-known for CMFD; the same procedure would apply to CQD.

The generalization of the CQD method to multi-dimensional geometries will require the use of Eddington tensors, rather than Eddington factors. (This is a necessary feature of QD simulations.)

We have noted that the CQD method derived in this paper is not the only way to make the QD "consistent;" this has been done in two previous publications [6,7]. In future work, it would be interesting to compare the performance of the earlier methods with the CQD method presented here. It would be especially interesting if the previous methods have better stability properties. This might suggest new ways to improve the stability of CMFD for coarser grids.

The analysis presented in this paper makes it possible to modify a QD (or VEF) code to have the potential, if the transport consistency factors are "turned on," to preserve the S_N solution. This capability would allow code users to investigate the accuracy of the QD approximation, for problems in which "transport effects," which degrade the accuracy of QD solutions, might be significant.

It would also be possible to use the CQD transport consistency factor *selectively*. To be specific, the consistency factor could be "turned on" in "transport" regions where transport effects are considered to be significant, and "turned off" (set to zero) in "diffusive" regions where transport effects are considered to be weak. (Effectively, the S_N equations would be solved in the "transport" regions, and the QD equations would be solved in the "diffusive" regions.) If the spatial grids in the "transport regions" are optically thin – as they should be, to resolve transport effects – then the resulting "partially consistent" QD method should have improved accuracy, with convergence rates comparable to standard QD.

In conclusion, the ability to make QD fully or partially consistent provides a new and possibly useful capability to code users. We hope to continue our work on this topic.

ACKNOWLEDGEMENTS

We would like to thank Dmitriy Anistratov for his helpful advice concerning previously-published work on "consistent" Quasidiffusion methods.

REFERENCES

[1] V.Ya. Gol'din, "A Quasi-Diffusion Method for Solving the Kinetic Equation," *USSR Comp. Math. and Math. Phys.* **4**, 136 (1967).

[2] G.R. Cefus and E.W. Larsen, "Stability Analysis of the Quasidiffusion and Second Moment Methods for Iteratively Solving Discrete Ordinates Problems," *Transport Th. Stat. Phys.* **18**, 493 (1990).

[3] M.L. Adams and E.W. Larsen, "Fast Iterative Methods for Discrete-Ordinates Particle Transport Calculations," *Prog. Nucl. Energy* **40**, 3 (2002).

[4] K.S. Smith and J.D. Rhodes, III, "Full-Core, 2-D, LWR Core Calculations with CASMO-4E," *Proc. PHYSOR 2002*, Seoul, Korea, (Oct. 7-10, 2002).

[5] E.W. Larsen and B.W. Kelley, "The Relationship Between the Coarse Mesh Finite Difference and the Coarse Mesh Diffusion Synthetic Acceleration Methods," *Nucl. Sci. Eng.* **178**, 1 (2014).

[6] D.Y. Anistratov, "Nonlinear Quasidiffusion Acceleration Methods with Independent Discretization," *Trans. Am. Nucl. Soc.* **95**, 553 (2006).

[7] E. Masiello, R. Sanchez, and I. Zmijarevic, "New Numerical Solution with the Method of Short Characteristics for 2-D Heterogeneous Cartesian Cells in the APOLLO2 Code: Numerical Analysis and Tests," *Nucl. Sci. Eng.* **161**, 257 (2009).